ACS APPLIED MATERIALS & INTERFACES

Letter

www.acsami.org

Zn_2GeO_4 Nanowires As Efficient Electron Injection Material for Electroluminescent Devices

Jiangxin Wang,[†] Chaoyi Yan,[†] Shlomo Magdassi,[‡] and Pooi See Lee*[,†]

[†]School of Materials Science and Engineering, Nanyang Technological University, 50 Nanyang Avenue, Singapore 639798

[‡]Institute of Chemistry, The Hebrew University of Jerusalem, Jerusalem 91904, Israel

Supporting Information

ABSTRACT: Pure phase Zn_2GeO_4 nanowires (NWs) were grown by the chemical vapor transport method on *p*-GaN: Mg/Al_2O_3 substrate. The as-grown Zn_2GeO_4 NWs exhibited n-type characteristic due to native defects and formed a p−n heterojunction with the p-GaN substrate. The unique energy level of Zn_2GeO_4 NWs promotes electron injection into GaN active region while suppressing hole injection into Zn_2GeO_4 NWs. The device exhibited an emission centered at 426 nm and a low turn-on voltage around 4 V. Zn_2GeO_4 NWs are first reported in this paper as promising electron transport and injection material for electroluminescent devices.

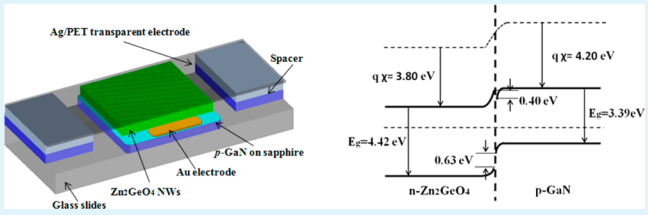

KEYWORDS: *zinc germinate nanowires, p-GaN, light emitting diode, electron injection, electroluminescence, p-n heterojunction*

1. INTRODUCTION

Nanowire electroluminescent devices have attracted extensive attention because of the many advantages of NWs, such as structural flexibility, high crystallinity, and nanoscale dimension. The unique one-dimensional structure of NWs provides a spontaneous mechanism for strain relaxation and lattice mismatch accommodation,[1] making it viable to integrate other functional materials onto III−V optically active semiconductors with low defects. This advantage helps to increase carrier injection efficiency and contribute in tackling the challenging problem of efficiency droop in light-emitting diode (LED), which is partially related to the high dislocation density caused by lattice-mismatch epitaxy.[2] Moreover, NWs provide direct pathways for photon transport, improved photon extraction is expected in the one-dimensional nanostructure. Apart from being used as the light emitting active elements, nanowires are also good candidates for carrier injection materials. The capability to grow high-crystal-quality nanowires on the substrates with less lattice match requirement[3−5] enables a large range of materials selection for carrier transport and injection, which opens up numerous freedoms to engineer band structures of the p−n junctions and improve the LEDs performance.

Zn_2GeO_4 is a ternary functional oxide with many unique and interesting properties, such as negative thermal expansion below room temperature,[6] white luminescence due to native defects,[7] and high photon response for ultraviolet light detection.[8] Earlier optoelectronic studies mainly focused on its properties in high field electroluminescence because of some of its advantages: extreme stability under high electrons irradiation, presence of native defects that act as effective emission centers and large bandgap that can avoid self-absorption of emitted light.[7,9−11] However, it is challenging to explore this material for application in LED devices in the bulk structure due to its relatively high resistivity (1×10^{11} Ohm cm based on bulk structure[12]) and large lattice mismatch with optically active III−V materials. In this work, we synthesized Zn_2GeO_4 single-crystal nanowires on III−V substrate and fabricate nanowire LED device using Zn_2GeO_4 nanowires as an efficient charge injection layer based on its unique band structure, efficient charge transport and tolerance to lattice mismatch. It was demonstrated that LED devices could be successfully fabricated by integrating Zn_2GeO_4 NWs with p-GaN substrate. The electrical and optical properties of Zn_2GeO_4 NWs in injection electroluminescent devices were elucidated.

2. EXPERIMENTAL SECTION

The Zn_2GeO_4 NWs were synthesized by a chemical vapor transport method.[13] ZnO, GeO_2, and carbon powders were mixed with molar ratio of 2:1:3. The mixed powder was put into a 30 mm diameter quartz tube and inserted into the furnace, which was heated up to 1000 °C. Ar gas mixed with 10% O_2 was used as carrier gas. Si substrates coated with thin Au film (∼10 nm) were used to collect NWs grown in the temperature region of 500−400 °C. The system pressure and oxygen concentration significantly affect morphology of the NWs (see Figure S1 in the Supporting Information). The growth conditions were chosen to achieve preferred NWs product based on the consideration of high electron injection efficiency and good carrier mobility. Detailed illustrations can be found in the Supporting Information. Morphology and

Received: April 5, 2013
Accepted: July 9, 2013
Published: July 9, 2013

   dx.doi.org/10.1021/am401234a | ACS Appl. Mater. Interfaces 2013, 5, 6793−6796

structures of the NWs were characterized by field-emission scanning electron microscopy (SEM, JEOL 7600F), transmission electron microscopy (TEM, JEOL 2100), and X-ray diffraction (XRD, Shimashu XRD-6000, Cu Ka radiation).

Mg-doped GaN (0001) epitaxial film (3 μm in thickness) on Al_2O_3 template was used as the *p*-type substrate. Zn_2GeO_4 NWs were grown on the substrate by the method described above. The GaN substrate was partially covered and protected by a hard mask during the nanowire growth process. After the Zn_2GeO_4 NW growth, 100 nm Au layer was sputtered onto the protected area and followed by a 500 °C rapid thermal annealing for 3 min in air to form Ohmic contact. The prepared sample was placed onto a glass slide which served as a supporting substrate. Two clean GaN substrates with thin elastic films (paraffin film) on top were put on both sides of the sample to serve as spacers. Bulldog clips were used to press Ag/PET transparent electrode onto the spacers and assemble the device.[14,15] By using this method, we can achieve good Ohmic contact between the top electrode and underneath NWs without complex processes of insulating layers deposition, plasma etching, and transparent electrode deposition.[16,17]

3. RESULTS AND DISCUSSION

Top view of the Zn_2GeO_4 NWs grown on p-GaN substrate is shown in Figure 1a. The lengths are typically ~100 μm with a

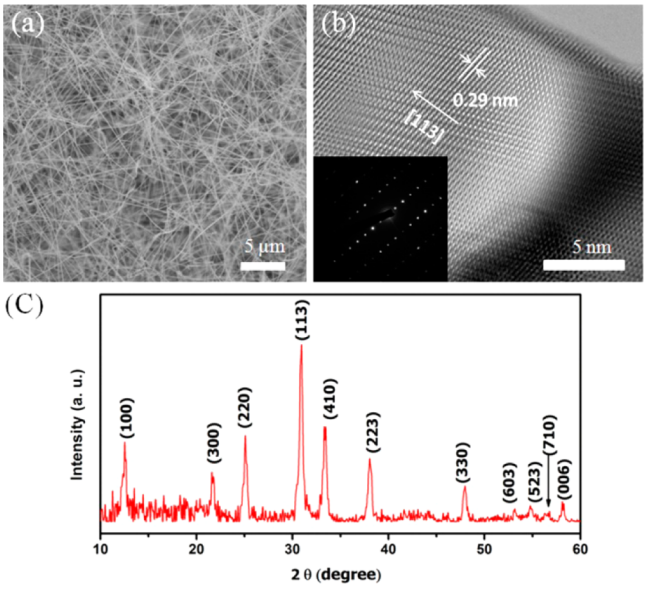

Figure 1. (a) SEM image of Zn_2GeO_4 NWs. (b) High-resolution TEM image of the Zn_2GeO_4 NWs, which have a growth direction of ⟨113⟩. Inset is the corresponding selective area diffraction patterns. (c) XRD pattern of the Zn_2GeO_4 NWs.

growth time of 20 min. Figure 1b is a high-resolution TEM image of the Zn_2GeO_4 NWs, showing single-crystalline structure of the NWs. Crystallinity of the NWs was further confirmed by the selective area electron diffraction (SAED) patterns, as shown in Figure 1b inset. Figure 1c is the XRD pattern of the Zn_2GeO_4 NWs. All the peaks can be readily indexed to a pure rhombohedral crystal phase (JCPDS: 011−0687, a = 14.231 Å, b = 9.53 Å). The high-purity Zn_2GeO_4 NWs eliminates the concern of impurity, such as ZnO NWs and GeO_2 NWs, which may affect performance of the devices.

Room-temperature photoluminescence (PL) of the Zn_2GeO_4 NWs on Si substrate and GaN substrate are presented in Figures 2a, b. The Zn_2GeO_4 NWs have a broad emission from

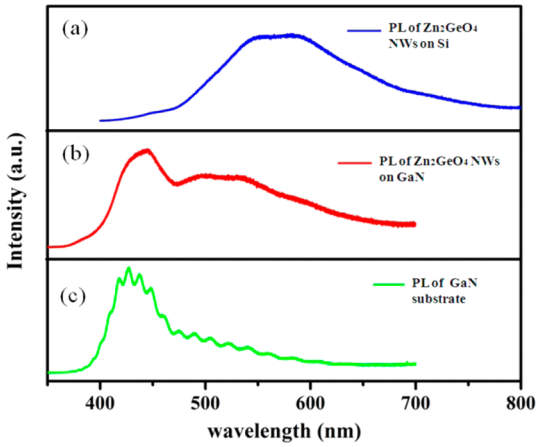

Figure 2. (a) Room-temperature PL spectrum of Zn_2GeO_4 NWs on Si substrate. (b) PL spectrum of Zn_2GeO_4 NWs on GaN substrate. (c) PL spectrum of pristine GaN substrate.

500 to 700 nm, which was ascribed to the donor−acceptor recombination from native defects.[7] Since the excitation energy (3.81 eV) was relatively low compared to the bandgap of Zn_2GeO_4 (4.42 eV), the band edge emission behavior of the NWs could not be shown. PL of the Zn_2GeO_4 NWs on GaN substrate was a combination of the narrow emission centered at ~440 nm and the broad emission from native defects of Zn_2GeO_4 NWs. The emission centered at ~440 nm came from the GaN substrate in which transits were from conduction band or shallow donors to the deep-level Mg dopants.[18] Figure 2c shows the PL from pristine GaN substrate, which confirms the 440 nm emission from GaN. The multipeaks structure in the spectrum was attributed to light interference in the GaN film.[19]

Figure 3a is a schematic of the Zn_2GeO_4 NW/*p*-GaN heterojunction device. Silver nanoparticles on PET substrate[20] (Ag/PET, sheet resistivity of 2 ohm/sq, transparency of ~65% from 900 to 370 nm) was used as the top transparent electrode by mechanical press onto the Zn_2GeO_4 NWs. Reliable current feeding and light extraction were achieved by this device configuration. Current−voltage (I−V) characteristic of the device was measured by a Keithley 4200 semiconductor analyzer. The device exhibited strong rectifying behavior with remarkable small reverse current, as presented in Figure 2b. Due to oxygen vacancy and zinc interstitial, as donors, the NWs behaved as intrinsic n-type materials.[21] The p−n heterojunction was formed between the Zn_2GeO_4 NWs and p-GaN substrate. Electrical properties of the device were further investigated by measuring the I−V characteristics under varied cryogenic temperature (see Figure S2 in the Supporting Information). It shows that Zn_2GeO_4 NWs had a carrier freeze-out temperautre at around 150 K. Detailed results and discussions are provided in the Supporting Information.

Strong blue emission from the device could be observed under forward bias, as shown in the inset of Figure 3c. No emission was detected under reverse bias. The emission spectra centered at 426 nm with a full width at half-maximum (fwhm) of about 60 nm, as shown in Figure 3c. The electroluminescence process can be explained by energy band diagram of the heterojunction in Figure 3d. The conduction band edge

dx.doi.org/10.1021/am401234a | ACS Appl. Mater. Interfaces 2013, 5, 6793−6796

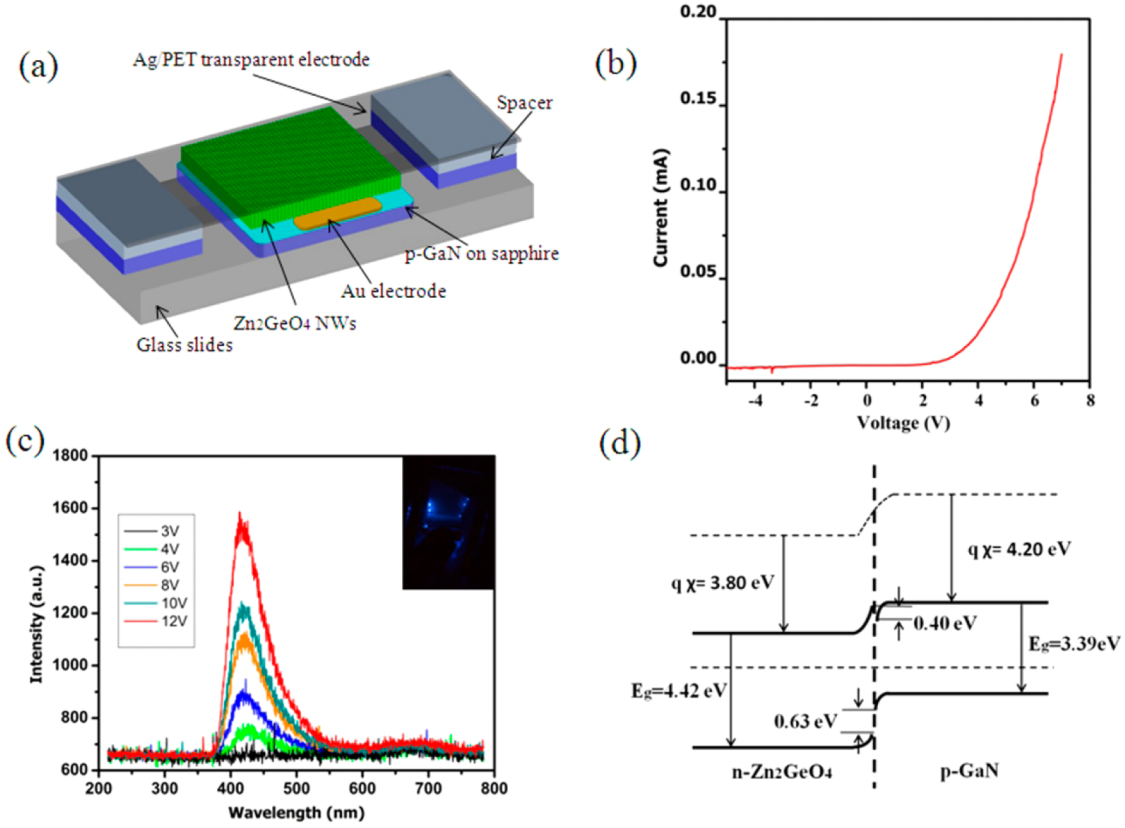

Figure 3. (a) Schematic of the Zn_2GeO_4 NWs/GaN heterojunction device. (b) Current−voltage curve of the LED device. (c) Electroluminescence spectra of synthesized device, inset is a lighted LED device under 10 V forward bias. (d) Energy band diagram of the heterojunction.

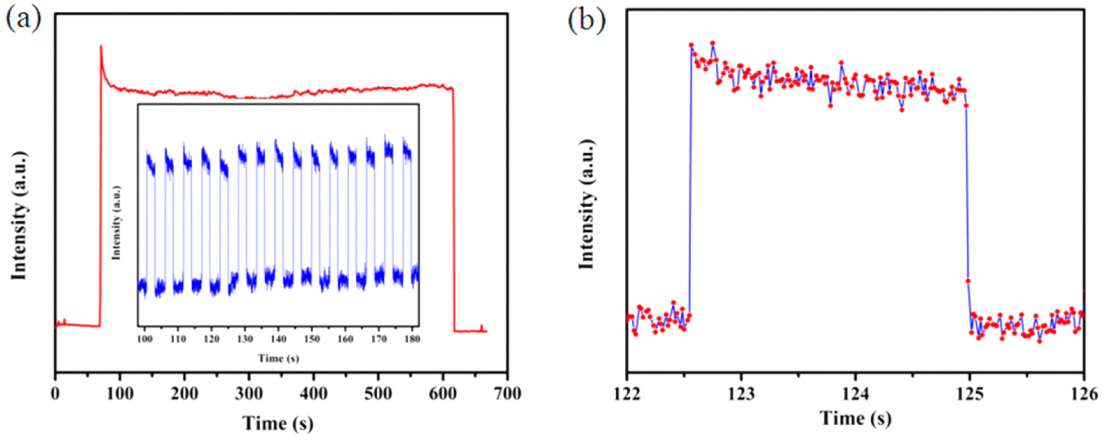

Figure 4. (a) EL stability test of the device with an operation time of 10 min under 8 V forward bias. Inset is the EL time respond of the device under rectangle pulse function. (b) Enlarged image for response of the device under a single pulse.

of Zn_2GeO_4 is located at around −3.80 eV (vs AVS-absolute vacuum state),[22] 0.4 eV higher than the conduction band of GaN (−4.20 eV vs AVS).[23] Electrons can be easily injected into GaN in this energy band structure.

It was reported that a Ga_2O_3 film formed on GaN substrates before the NWs growth in a chemical vapor deposition process. The Ga_2O_3 barrier reduced electron injection efficiency under forward bias and largely increased the turn on voltage of the LED device to +11.5 V.[24] The large turn-on voltage was not observed in our devices which have a low turn-on voltage at around 4 V. This suggests that the Zn_2GeO_4 NWs should be in direct contact with GaN thin film and high quality heterojunction was formed in the device. The ease of electron injection greatly enhanced the minority carrier concentrations in the GaN active regions under forward bias, which increased the radiative recombination rate while the nonradiative recombination rate may be suppressed due to saturation of deep level traps.[25] There is a 0.63 eV energy barrier (ΔE_v = 0.63 eV) between the valence bands of Zn_2GeO_4 and GaN. Hole injection into the conduction band of Zn_2GeO_4 NWs is largely suppressed under the high energy barrier. Because of the low injection efficiency, these minority carriers more likely relaxed through nonradiative recombination process. Consequently, no characteristic emission from Zn_2GeO_4 NWs was observed in the EL spectra. No emission was detected from the device with forward voltage below 3 V. When the bias was

dx.doi.org/10.1021/am401234a | ACS Appl. Mater. Interfaces 2013, 5, 6793−6796

increased to 4 V, slightly above the bandgap of GaN, high electrons injection took place, resulting in emission from the GaN centered at 426 nm. The low turn-on voltage was attributed to good Ohmic contact in the device and high quality interface at the nanocontact of Zn_2GeO_4 NWs and GaN film.

Dynamic switching experiments were also performed to investigate stability and time response of the devices, as presented in Figure 4. Emission intensity of the device was quite stable during the test with 8 V forward bias. In order to test the time response behaviors, a rectangular pulse function (pulse width of 2.5 s, pulse period of 5 s and pulse voltage of 8 V) was applied to the device. As shown in Figure 4a inset, the device showed quick and repeatable response to the pulse function. The response time was below 16 ms, which was limited by the acquisition time of our spectrometer, as presented in one enlarged cycle in Figure 4b.

4. CONCLUSION

In conclusion, we demonstrate that the wide-bandgap intrinsic n-type ternary material, Zn_2GeO_4 NWs, can be used to form high quality p−n heterojunction with p-type GaN for electroluminescent applications. The conduction band offset (from Zn_2GeO_4 to GaN) ΔE_c is −0.4 eV, whereas the valence band offset ΔE_v is 0.63 eV. The p−n heterojunction greatly facilitates electron injection into p-GaN active materials while suppressing hole injection into Zn_2GeO_4. As a result, main radiative recombination process was confined in GaN active region, which has high internal quantum efficiency. The large bandgap of Zn_2GeO_4 NWs also reduces self-absorption of the emission and increases light extraction efficiency. Therefore, the ternary oxide NWs are promising materials for electroluminescent devices as electron injection layers.

■ ASSOCIATED CONTENT

Supporting Information

Additional figures and details (PDF). This material is available free of charge via the Internet at http://pubs.acs.org.

■ AUTHOR INFORMATION

Corresponding Author

*E-mail: pslee@ntu.edu.sg..

Notes

The authors declare no competing financial interest.

■ ACKNOWLEDGMENTS

This work is supported in part by the National Research Foundation Create Programme: Nanomaterials for Energy and Water Management, and Institute of Sports Research, NTU. The authors thank Dr. J. Yan for his insightful discussions and Ms. W. L. Foo for supply of Ag/PET transparent substrate. We also thank Dr. M. Yang and Dr. D. Zhang for their kind technical support.

■ REFERENCES

(1) Yang, P.; Yan, R.; Fardy, M. *Nano Lett.* **2010**, *10*, 1529−1536.
(2) Guo, W.; Zhang, M.; Banerjee, A.; Bhattacharya, P. *Nano Lett.* **2010**, *10*, 3355−3359.
(3) Martensson, T.; Svensson, C. P. T.; Wacaser, B. A.; Larsson, M. W.; Seifert, W.; Deppert, K.; Gustafsson, A.; Wallenberg, L. R.; Samuelson, L. *Nano Lett.* **2004**, *4*, 1987−1990.
(4) Kuykendall, T.; Ulrich, P.; Aloni, S.; Yang, P. *Nat. Mater.* **2007**, *6*, 951−956.
(5) Calarco, R.; Meijers, R. J.; Debnath, R. K.; Stoica, T.; Sutter, E.; Lüth, H. *Nano Lett.* **2007**, *7*, 2248−2251.
(6) Stevens, R.; Woodfield, B. F.; Boerio-Goates, J.; Crawford, M. K. *J. Chem. Thermodyn.* **2004**, *36*, 349−357.
(7) Liu, Z.; Jing, X.; Wang, L. *J. Electrochem. Soc.* **2007**, *154*, H500−H506.
(8) Yan, C.; Singh, N.; Lee, P. S. *Appl. Phys. Lett.* **2010**, *96*, 053108.
(9) Anoop, G.; Mini Krishna, K.; Jayaraj, M. K. *J. Alloys Compd.* **2009**, *468*, 512−515.
(10) Anoop, G.; Krishna, K. M.; Jayaraj, M. K. *J. Electrochem. Soc.* **2008**, *155*, J7−J10.
(11) Lewis, J. S.; Holloway, P. H. *J. Electrochem. Soc.* **2000**, *147*, 3148−3150.
(12) Struck, C. W.; Mishra, K. C.; Bartolo, B. D. *Physics and Chemistry of Luminescent Materials*; The Electrochemical Society: Pennington, NJ, 1999; p 142.
(13) Yan, C.; Lee, P. S. *J. Phys. Chem. C* **2009**, *113*, 14135−14139.
(14) Lupan, O.; Pauporte, T.; Viana, B. *Adv. Mater.* **2010**, *22*, 3298−3302.
(15) Lupan, O.; Pauporté, T.; Viana, B. *J. Phys. Chem. C* **2010**, *114*, 14781−14785.
(16) Xu, S.; Xu, C.; Liu, Y.; Hu, Y.; Yang, R.; Yang, Q.; Ryou, J. H.; Kim, H. J.; Lochner, Z.; Choi, S.; Dupuis, R.; Wang, Z. L. *Adv. Mater.* **2010**, *22*, 4749−4753.
(17) Zhang, X.-M.; Lu, M.-Y.; Zhang, Y.; Chen, L.-J.; Wang, Z. L. *Adv. Mater.* **2009**, *21*, 2767−2770.
(18) Alivov, Y. I.; Van Nostrand, J. E.; Look, D. C.; Chukichev, M. V.; Ataev, B. M. *Appl. Phys. Lett.* **2003**, *83*, 2943.
(19) Dai, J.; Xu, C. X.; Sun, X. W. *Adv. Mater.* **2011**, *23*, 4115−4119.
(20) Layani, M.; Magdassi, S. *J. Mater. Chem.* **2011**, *21*, 15378−15382.
(21) Liu, Z.; Liang, B.; Chen, G.; Yu, G.; Xie, Z.; Gao, L.; Chen, D.; Shen, G. *J. Mater. Chem. C* **2013**, *1*, 131−137.
(22) Liu, Q.; Zhou, Y.; Kou, J.; Chen, X.; Tian, Z.; Gao, J.; Yan, S.; Zou, Z. *J. Am. Chem. Soc.* **2010**, *132*, 14385−14387.
(23) Jeong, M.-C.; Oh, B.-Y.; Ham, M.-H.; Myoung, J.-M. *Appl. Phys. Lett.* **2006**, *88*, 202105.
(24) Yang, H. Y.; Yu, S. F.; Liang, H. K.; Lau, S. P.; Pramana, S. S.; Ferraris, C.; Cheng, C. W.; Fan, H. J. *ACS Appl. Mater. Interfaces* **2010**, *2*, 1191−1194.
(25) Mueller, G. *Electroluminescence I*; Academic Press: San Diego, CA, 2000; p 15.